

# Dynamic Simulation Model of Switched Reluctance Generator

Osamu Ichinokura, *Member, IEEE*, Tsukasa Kikuchi, Kenji Nakamura, *Member, IEEE*, Tadaaki Watanabe, *Member, IEEE*, and Hai-Jiao Guo, *Member, IEEE*

**Abstract**—This paper deals with a numerical model of the switched reluctance generator (SRG) for use on a general-purpose circuit simulation program “SPICE.” In the model, the electric circuit and magnetic circuit are coupled by proper controlled sources. Using the numerical model, we can readily calculate the dynamic behavior of the SRG. The method presented here is useful for circuit analysis and design optimization of the SRG.

**Index Terms**—switched reluctance generator (SRG), numerical model, SPICE simulation, dynamic characteristics.

## I. INTRODUCTION

THE SWITCHED reluctance motor (SRM) has desirable features including simple and solid construction, ease of maintenance, small moment of inertia, and low cost, because the SRM has no rotor windings and no permanent magnet. On the other hand, the SRM has the disadvantages of acoustic noise and torque ripple due to its salient-pole structure. So the applications of SRM were confined to a particular use, such as starters and fuel pumps of airplanes. In recent years, however, the disadvantages of SRM have been removed by the accurate control of driving circuit with the advance of power electronics technology [1]–[3]. Then, it is expected that SRM will have a growing applications in the future.

The features of SRM mentioned above show that the application of SRM to a generator is interesting. The solid construction is useful for ultrahigh-speed generator such as a microgas turbine generator. On the other hand, simple structure and a small moment of inertia suit a low-speed multipolar generator for use in wind-turbine generation. Several papers have reported on the application of SRM to a generator [4]–[6]. Few papers, however, have reported quantitative analysis of dynamic characteristics of the switched reluctance generator (SRG).

In the previous paper, the authors proposed a numerical model of SRM for use on the general-purpose circuit simulation program “SPICE” [7], [8]. Using the model, we can readily calculate the dynamic characteristics of SRM. On the basis of the SRM model, we present a method for analysis of dynamic characteristics of SRG in this paper.

Manuscript received January 2, 2003. This work was supported in part by the Grant in Aid for Scientific Research (C) 13650294.

The authors are with the Department of Electrical and Communication Engineering, Tohoku University, Aoba, Sendai 980-8579, Japan (e-mail: [ichinoku@ecei.tohoku.ac.jp](mailto:ichinoku@ecei.tohoku.ac.jp); [kikuchi@power.ecei.tohoku.ac.jp](mailto:kikuchi@power.ecei.tohoku.ac.jp); [nakaken@ecei.tohoku.ac.jp](mailto:nakaken@ecei.tohoku.ac.jp); [watanabe@ecei.tohoku.ac.jp](mailto:watanabe@ecei.tohoku.ac.jp); [kaku@ecei.tohoku.ac.jp](mailto:kaku@ecei.tohoku.ac.jp)).

Digital Object Identifier 10.1109/TMAG.2003.816739

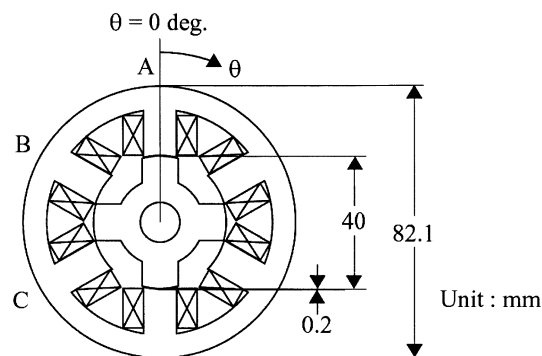


Fig. 1. Basic structure of SRG.

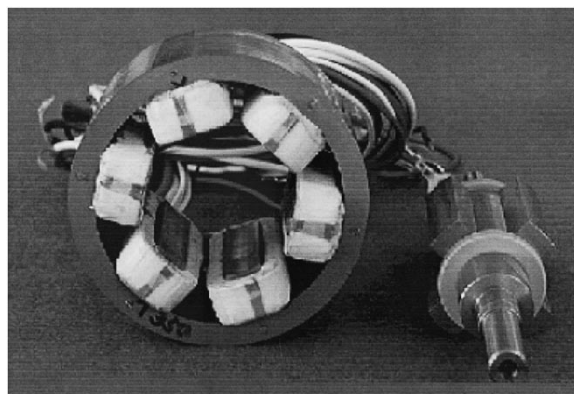


Fig. 2. General view of the SRG.

## II. BASIC OPERATION AND NUMERICAL MODEL OF SRG

Fig. 1 illustrates a basic structure of SRG used in this paper and Fig. 2 shows a general view of the SRG. The core material is nonoriented silicon steel with a thickness of 0.35 mm. The stack length is 51 mm, the stator pole arc is  $30^\circ$ , and the rotor pole arc is  $32^\circ$ . The number of turns in the winding is 72 per phase.

Now, let the rotor position angle be  $\theta$ , which is  $0^\circ$  when the rotor is in the aligned position relative to the phase A stator pole, as shown in Fig. 1.

Fig. 3 sketches the relationship between the winding inductance  $L$  of the phase A and the rotor position angle  $\theta$ . The torque  $\tau$  is given by

$$\tau = \frac{1}{2} i^2 \frac{dL}{d\theta}. \quad (1)$$

Then, the torque is negative in the region of  $dL/d\theta < 0$ . When the rotor is driven by a proper prime mover and the stator wind-

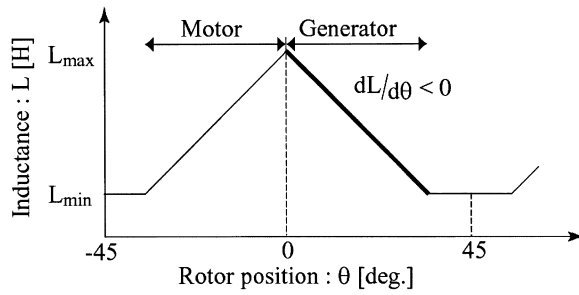


Fig. 3. Inductance versus rotor position curve.

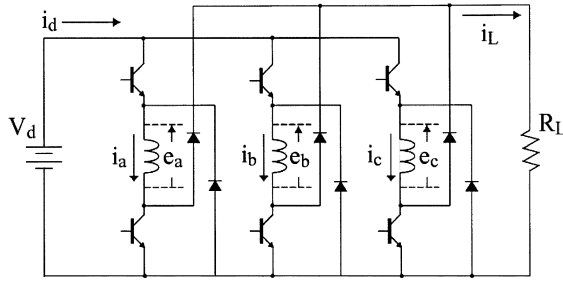


Fig. 4. Basic circuit of the SRG.

ings are excited in the region, the mechanical energy by the prime mover can be transformed into electric energy.

Fig. 4 shows a basic circuit of the SRG. The stator windings are excited by a conventional converter with two switches per phase. The generated electric power is supplied to the external load resistance  $R_L$ .

Now, we obtain the simulation model of the SRG under a simple assumption that the magnetic saturation and iron losses of the stator and rotor cores are neglected. Then the SRG can be expressed by a variable reluctance circuit in the same manner as SRM. Fig. 5 shows the model of SRG per phase. In the figure,  $R(\theta)$  shows the variable reluctance for expressing the SRG and is determined based on FEM analysis [7].  $Ni$  is a voltage source controlled by the exciting current and  $e'$  is a induced voltage given by  $e' = N(d\phi/dt)$ . The center circuit gives the induced voltage. The winding resistance is  $r$  and  $R_L$  is the load resistance.

Fig. 6 shows a flow diagram of the calculation. Here, we assume that the SRG is driven by a prime mover with constant rotational speed characteristic. When the rotational angular velocity  $\omega$  is given, the rotor position angle  $\theta$  is calculated by  $\theta = \int \omega dt$ . Then the voltages and currents of SRG are calculated by the main circuit.

Using the exciting currents  $i_a, i_b, i_c$  and  $dL(\theta)/d\theta$ , which is obtained by  $R(\theta)$  curves, we can calculate the generator torque  $\tau$ . The motion equation is

$$J \frac{d\omega}{dt} = \tau - \tau_L. \quad (2)$$

When the angular velocity is constant, the external torque  $\tau_L$  is equal to the generator torque  $\tau$ . Then, the mechanical input power is given by

$$P_m = \frac{1}{T} \int_0^T \omega \cdot \tau dt. \quad (3)$$

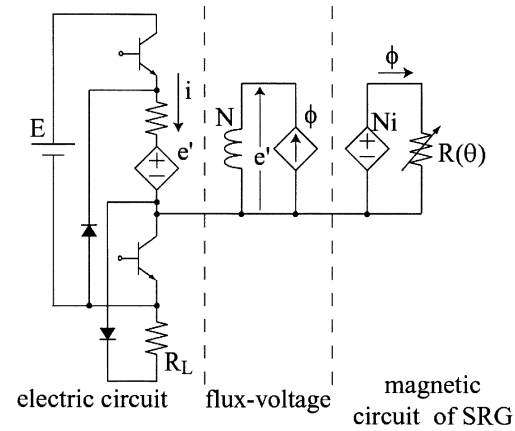


Fig. 5. Simulation model of the main circuit of SRG.

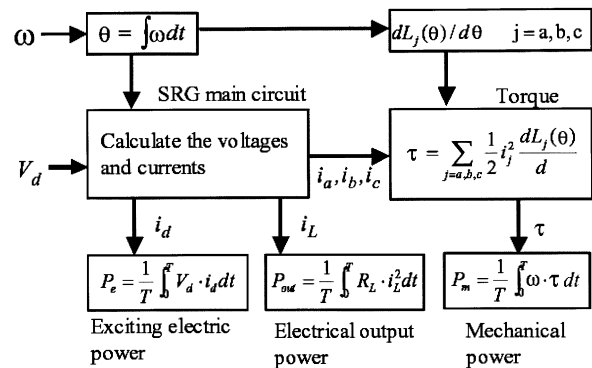


Fig. 6. Flow diagram of the calculation.

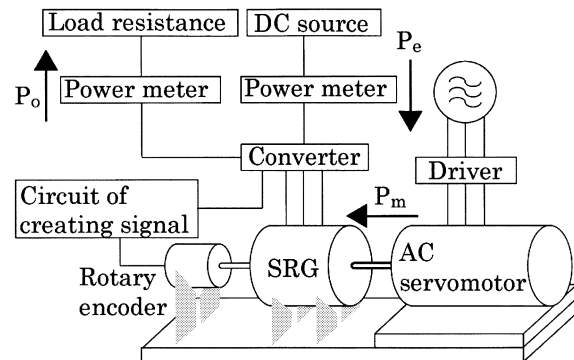


Fig. 7. Schematic layout of the experimental system.

The exciting electric power  $P_e$  and output power  $P_o$  are

$$P_e = \frac{1}{T} \int_0^T V_d \cdot i_d dt \quad (4)$$

$$P_o = \frac{1}{T} \int_0^T R_L \cdot i_L^2 dt. \quad (5)$$

### III. SIMULATION AND EXPERIMENTAL RESULTS

Based on the above considerations, we calculate the basic characteristics of SRG and compare the experimental results. Fig. 7 shows a schematic layout of the experimental system. The SRG is driven by an induction motor.

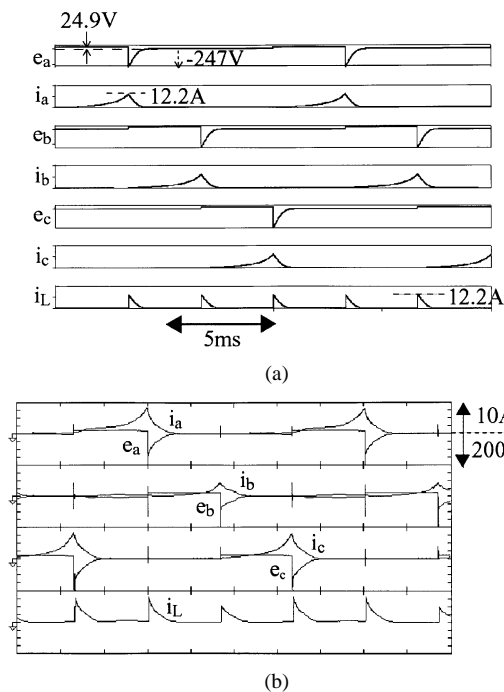


Fig. 8. Calculated and observed waveforms of the SRG.

Fig. 8 shows a simulation and experimental results of operating waveforms of the SRG at the direct-current (dc) voltage  $V_d = 25$  V, revolution speed  $N_r = 1500$  r.p.m., and load resistance  $R_L = 20 \Omega$ . In the figure,  $e_a, e_b, e_c$  and  $i_a, i_b, i_c$  are the winding voltages and currents of the phases A, B, C, respectively. The load current is  $i_L$ . This reveals that the large voltages with reversed polarity are generated in the windings and the electric power is supplied to the load resistance when the transistors are turned off. Although the quantitative errors cannot be disregarded, the tendency of the calculated waveforms agree with the experimental ones.

Fig. 9 shows the calculated and experimental results of the power-conversion characteristics at  $N_r = 1500$  rpm and  $R_L = 20 \Omega$ . In this figure,  $P_m, P_e$ , and  $P_o$  are the mechanical, exciting, and output powers, respectively. As the input energy of SRG is not only mechanical power, but also exciting electric power, we define the efficiency by  $\eta = 100 \times P_o / (P_m + P_e)$  [%]. It reveals that the calculated and experimental values show a similar tendency. The differences between the calculated

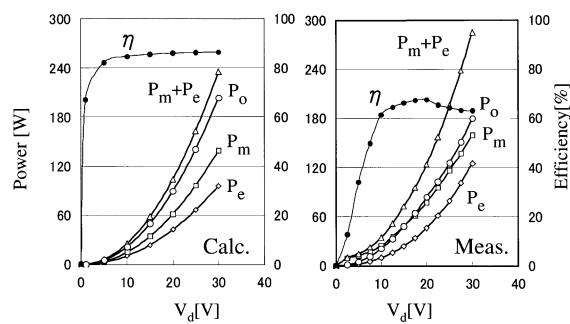


Fig. 9. Power-conversion characteristics of the SRG.

and measured values are caused by neglecting the iron losses and mechanical losses of SRG and neglecting the magnetic saturation of the stator and rotor cores in the calculations.

#### IV. CONCLUSION

The numerical model of SRG proposed here is useful for analysis and design of SRG. Furthermore, the model can be easily applied to the system simulation such as a wind-turbine generation by considering the output characteristic of the windmill. The application to the system simulation and improvement of preciseness of calculated values are under investigation now.

#### REFERENCES

- [1] P. J. Lawrenson, J. M. Stephanson, P. T. Blebkinsop, J. Corda, and N. N. Fulton, "Variable-speed switched reluctance motors," *Inst. Elect. Eng. Proc.*, vol. 127, pp. 253–265, 1980. Pr. B.
- [2] R. C. Becerra, M. Ehsani, and T. J. E. Miller, "Commutation of SR motors," *IEEE Trans. Power Electron.*, pp. 257–263, July 1993.
- [3] T. A. Lipo and Y. Li, "The CFM—A new family of electrical machines," in *Proc. IPEC-Yokohama'95*, 1995, pp. 1–9.
- [4] E. Richter and C. Ferreira, "Performance evaluation of a 250 kW switched reluctance starter generator," in *Conf. Rec. 1995 IEEE Industry Applicat.*, vol. 1, 1995, pp. 434–440.
- [5] M. Abouzeid, "The use of an axial field-switched reluctance generator driven by wind energy," *Renewable Energy*, vol. 6, pp. 619–622, 1995.
- [6] R. Cardenas-Dobson, G. M. Asher, and W. F. Ray, "Experimental evaluation of a switched reluctance generator for wind energy application," *Wind Eng.*, vol. 20, pp. 115–136, 1996.
- [7] O. Ichinokura, S. Suyama, T. Watanabe, and H. J. Guo, "A new calculation model of switched reluctance motor for use on SPICE," *IEEE Trans. Magn.*, vol. 37, pp. 2834–2836, July 2001.
- [8] T. Tsukii, K. Nakamura, and O. Ichinokura, "SPICE simulation of SRM considering nonlinear magnetization characteristics," *Elect. Eng. Jpn.*, vol. 142, pp. 16–21, 2003.